Heliyon 10 (2024) e31207

Contents lists available at ScienceDirect

Heliyon

journal homepage: www.cell.com/heliyon

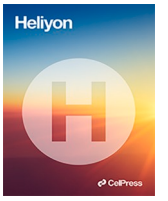

Research article

T cell-mediated tumor killing based signature to predict the prognosis and immunotherapy for glioblastoma

Hongchao Liu *, Kangke Shi, Zhihao Wei, Yu Zhang, Jiaqiong Li

Department of Pathology, The Yiluo Hospital of Luoyang, The Teaching Hospital of Henan University of Science and Technology, Luoyang, China

ARTICLE INFO

Keywords:
Glioblastoma
T cell-mediated tumor killing
Signature
Prognosis
Immunotherapy

ABSTRACT

Despite the significant advancements in cancer treatment brought by immune checkpoint inhibitors (ICIs), their effectiveness in treating glioblastoma (GBM) remains highly dissatisfactory. Immunotherapy relies on the fundamental concept of T cell-mediated tumor killing (TTK). Nevertheless, additional investigation is required to explore its potential in prognostic prediction and regulation of tumor microenvironment (TME) in GBM. TTK sensitivity related genes (referred to as GSTTKs) were obtained from the TISIDB. The training cohort was available from the TCGA-GBM, while the independent validation group was gathered from GEO database. Firstly, we examined differentially expressed GSTTKs (DEGs) with limma package. Afterwards, the prognostic DEGs were identified and the TTK signature was established with univariate and LASSO Cox analyses. Next, we examined the correlation between the TTK signature and outcome of GBM as well as immune phenotypes of TME. Furthermore, the evaluation of TTK signature in predicting the effectiveness of immunotherapy has also been conducted. We successfully developed a TTK signature with an independent predictive value. Patients who had a high score experienced a worse prognosis compared to patients with low scores. The TTK signature showed a strong positive association with the infiltration degree of immunocyte and the presence of various immune checkpoints. Moreover, individuals with a lower score exhibited increased responsiveness to ICIs and experienced improved prognosis. In conclusions, we successfully developed and verified a TTK signature that has the ability to predict the outcome and immune characteristics of GBM. Furthermore, the TTK signature has the potential to direct the personalized immunotherapy for GBM.

1. Introduction

Glioblastoma (GBM) is the predominant form of intracranial malignant tumor. GBM patients typically experience a poor outcome, and the current median survival is only about 12 months [1]. Currently, the primary approach for treating GBM involves surgery, subsequent radiation therapy, chemotherapy, and targeted therapy [2,3]. Despite the utilization of extensive therapeutic approaches, the prognosis for individuals with GBM remains exceedingly unfavorable, with nearly all patients experiencing a recurrence of GBM [4,5]. Hence, there is an urgent need for more efficient approaches to treat GBM.

GBM has benefited from the widespread utilization of immune checkpoint inhibitors (ICIs) in the treatment of various malignant tumors, offering innovative therapeutic approaches in recent times [6–8]. ICIs therapy, in contrast to conventional cytotoxic

* Corresponding author.
E-mail address: lhongchao@hotmail.com (H. Liu).

https://doi.org/10.1016/j.heliyon.2024.e31207
Received 8 August 2023; Received in revised form 8 May 2024; Accepted 13 May 2024
Available online 14 May 2024

chemotherapy, eradicates cancer cells by specifically targeting checkpoint molecules and rejuvenating immune cell functions [9]. While ICIs have revolutionized the field of tumor treatment, the therapeutic effect for GBM by ICIs is very unsatisfying. The response to ICIs is influenced by immune cells, stromal cells, and different cytokines present in tumor microenvironment (TME), which are considered crucial factors. T cell sub-groups display a central role in fighting against tumors, and the fundamental concept of immunotherapy is the destruction of tumors through T cell-mediated tumor killing (TTK) [10,11]. GBM exhibits a significantly high level of immunosuppression. The immunosuppressive condition is caused by tumor cell-derived suppressive substances, which restrict the activation of immune cells that fight against tumors, lead to exhaustion of activated T-cells, and induce inhibitory impacts on the antitumor immunity [12,13]. Therapy resistance in GBM patients, which includes tumor heterogeneity and immune dysfunction, has also been a major factor contributing to the limited advantages of ICIs treatment [14]. Although the clinical trials about ICIs in GBM have showed disappointing results, there is currently significant interest in improving outcomes by combining ICIs with other therapeutic approaches.

Up until now, a comprehensive examination of genes associated with TTK in GBM has not been conducted. The precise role of TTK in GBM and its associations with clinical outcomes and immunotherapy remain poorly understood. Hence, in this research, we initially created and verified an innovative TTK signature through comprehensive examination of gene expression information from several separate groups of GBM individuals. The TTK signature appears to be strongly associated with clinical results and the immune status of TME, enabling it to predict the immunotherapy reaction in GBM patients.

2. Materials and methods

2.1. Datasets acquisition

To begin, we obtained the training cohort from the TCGA-GBM dataset [15]. GBM samples missing clinical data were excluded. Following the preprocessing of data, the training cohort for TCGA-GBM comprised of 143 patients and an additional five controls. The validation cohort, GSE121720, consisting of 58 samples of GBM and four samples of normal tissue, was acquired from the GEO repository [16]. The gene symbols were obtained by converting the array probes in the GSE121720 dataset using annotation files. Excluded were the probes that targeted multiple genes, and the expression levels was averaged if multiple probes were mapped to a single gene.

GSTTKs, which are genes that regulate the sensitivity to T cell-mediated tumor killing, were acquired from TISIDB [17]. 607 GSTTKs were summarized for further analysis after eliminating duplicates.

2.2. Screening of differentially expressed GSTTKs

To begin with, the 'limma' was employed to identify differentially expressed GSTTKs (DEGs) in GBM and normal samples [18]. DEGs with a $|\log_2(\text{fold change})| > 0.585$ and corrected P-value < 0.05 were deemed statistically significant. Next, the 'ClusterProfiler' was used to conduct Gene Ontology (GO) and pathway enrichment analyses [19]. Moreover, the network of protein-protein interactions (PPI) for these DEGs was established utilizing the STRING and presented with Cytoscape (v3.9.1) [20].

2.3. Development and validation of the TTK signature

Initially, we conducted univariate analysis in the TCGA-GBM cohort to identify DEGs associated with prognosis. Next, the 'glmnet' was adopted to preform LASSO analysis on the prognostic DEGs [21]. The ideal lambda was assessed through a 95 % confidence interval (CI) and established using a ten fold cross-validation. The TTK model was created according to the selected gene's expression and coefficients, which meant that the score was computed by multiplying the gene expression with the regression coefficients and then summing them up.

Next, the TTK score was calculated for every GBM patient, and subsequently, the patients were classified into two groups using the TTK score median. Survival curve was generated with the 'survminer' package, and the log-rank survival test was used to compare the differences in mortality between two groups. Furthermore, we generated ROC curves utilizing the 'timeROC' package, and evaluated the predictive accuracy and effectiveness of the TTK signature by calculating the AUC. Additionally, the validation of the TTK signature's predictive role was carried out in the GSE121720 cohort.

2.4. Establishment of the nomogram

Cox regression models were used to select the clinical predictors of outcome. Moreover, we integrated prognostic elements into a unified nomogram to estimate the likelihood of survival for GBM patients utilizing the 'rms' R software package. Calibration curve of the diagnostic nomogram was used to quantify the statistical effectiveness.

2.5. Evaluation of immune characteristics

The 'GSVA' package was used to apply the single sample gene set enrichment analysis (ssGSEA) algorithm on the RNA sequencing data of TCGA-GBM dataset, and this analysis quantified the infiltration degree of immunocyte [22,23]. The enrichment scores of immunocyte were compared with Wilcoxon test. Spearman analysis was also conducted to investigate the potential association

between signature genes and the immunocyte infiltration. Furthermore, we also assessed the diversity in immune checkpoints expression between two groups.

2.6. Prediction of the clinical response to immunotherapy

The evaluation of the patients' reaction to ICIs treatment was conducted using the cohort associated with immunotherapy, and the raw data for the Gide_CancerCell_pre cohort were obtained from GitHub [24]. The Tumor Immune Dysfunction and Exclusion (TIDE) algorithm was employed to evaluate the response to immunotherapy [25].

2.7. Molecular docking to screen candidate compounds

The Protein Data Bank (PDB) was used to download protein structures, while the DrugBank database provided the structure data files for compounds [26]. The compounds were first filtered based on Lipinski's rules, and non-drug-like compounds were discarded. The molecular docking was performed with AutoDock-Vina program, and the Pumol software was utilized to visualize the binding of compounds to proteins [27].

2.8. Statistical analysis

R software (Version 4.1.2) was utilized for performing statistical analyses and visualization. *Pearson* analysis was employed to evaluate the associations among continuous variables. The Wilcoxon test was applied to compare continuous variables between two groups. The Kruskal-Wallis test was used to evaluate a comparison of multiple groups of continuous variables. Statistically significant analyses were those with a two-sided P value < 0.05.

3. Results

3.1. Screening of differential GSTTKs and functional analysis

A total of 561 GSTTKs were identified in the expression profiles of the TCGA-GBM dataset. The volcano plot illustrated the changes in GSTTKs expression between GBM and normal samples, with the figure labeling the top ten GSTTKs that were up- and down-regulated (Fig. 1A). According to the data presented in Fig. 1B, GBM samples exhibited significantly elevated expression levels of PCBP2, FOXM1, and ANG genes, whereas normal samples showed significantly higher expression levels of USP31, KIF3A, and MBNL2 genes. Fig. 1C demonstrated the remarkable distinction between tumor and controls through principal component analysis (PCA) on these 561 GSTTKs.

Using the 'limma' R package, we conducted a differential analysis in TCGA-GBM dataset. As a result, we identified 6699 genes that showed differential expression in GBM and normal samples, based on the aforementioned thresholds. From the intersection of 561 GSTTKs, we identified 226 GSTTKs that showed differential expression. 177 GSTTKs were found to be overexpressed, while 49 GSTTKs were downregulated in patients (Supplementary Table S1). Next, we examined the association between 226 DEGs and clinicopathological characteristics of GBM patients. According to the age and original subtype, the findings revealed that GPX8 exhibited differential expression in subgroups, while TIMP1 showed differential expression in subgroups based on the IDH status and original subtype (Supplementary Figs. S1–S5 and Supplementary Table S2).

The DEGs were mainly enriched in ribosome assembly, antigen presentation, and cytoplasmic translation during the GO-biological process analysis (Fig. 2A). In the GO-cellular component analysis, the DEGs were found to be enriched in cell-substrate junction, focal

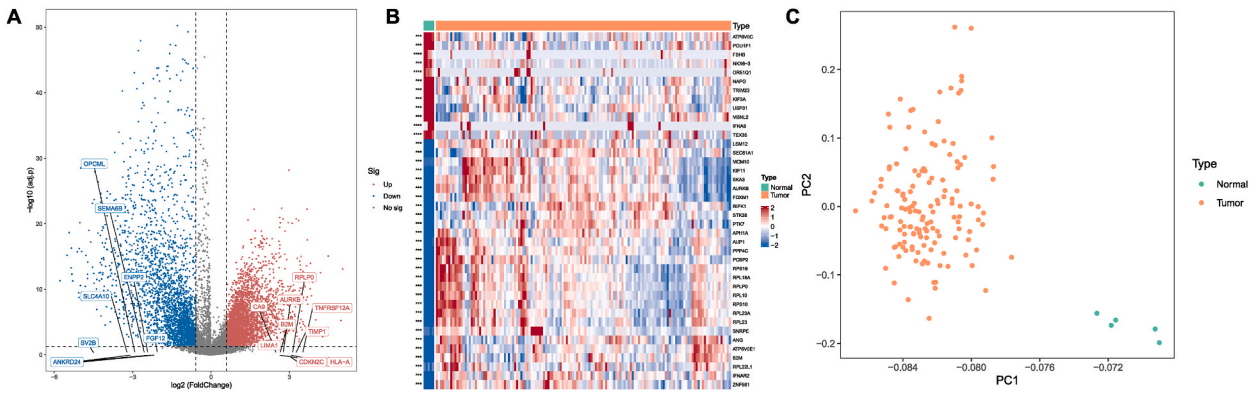

Fig. 1. The expression analysis of GSTTKs in GBM expression profile from TCGA.
A. Volcano plot showing the genes expression differences in GBM and normal specimens. B. Heatmap of the top 40 significantly differential GSTTKs in GBM and normal specimens. C. PCA for GBM and normal specimens.

adhesion, and ribosome (Fig. 2B). DEGs in the GO-molecular function analysis were enriched in ribosome structural constituent, transcription factor binding, rRNA binding, and tumor necrosis factor receptor binding (Fig. 2C). Furthermore, the KEGG analyses revealed that the DEGs showed enrichment in the ribosome, antigen processing and presentation, and the Toll-like receptor pathway (Fig. 2D). According to the analysis of the PPI network, RPLP0, MYC, and RPL35A potentially have a significant impact on TTK-related pathways in GBM (Supplementary Fig. S6).

3.2. Development and verification of TTK signature for GBM

Initially, we discovered 20 genes associated with prognosis by conducting univariate Cox model on the 226 DEGs in the TCGA-GBM cohort. Furthermore, we conducted LASSO regression using these 20 prognostic genes. A simplified prediction model was constructed using 14 selected genes, with a lambda value of 0.032 considered optimal (Fig. 3A and B). The TTK signature for GBM was ultimately determined based on 14 GSTTKs (Fig. 3C and Supplementary Table S3). Survival curve was generated using the Kaplan-Meier technique to evaluate the prognostic significance (Fig. 3D–I).

Within the TCGA-GBM cohort, patients were categorized into two groups with the median score as the dividing factor (Fig. 4A–C).

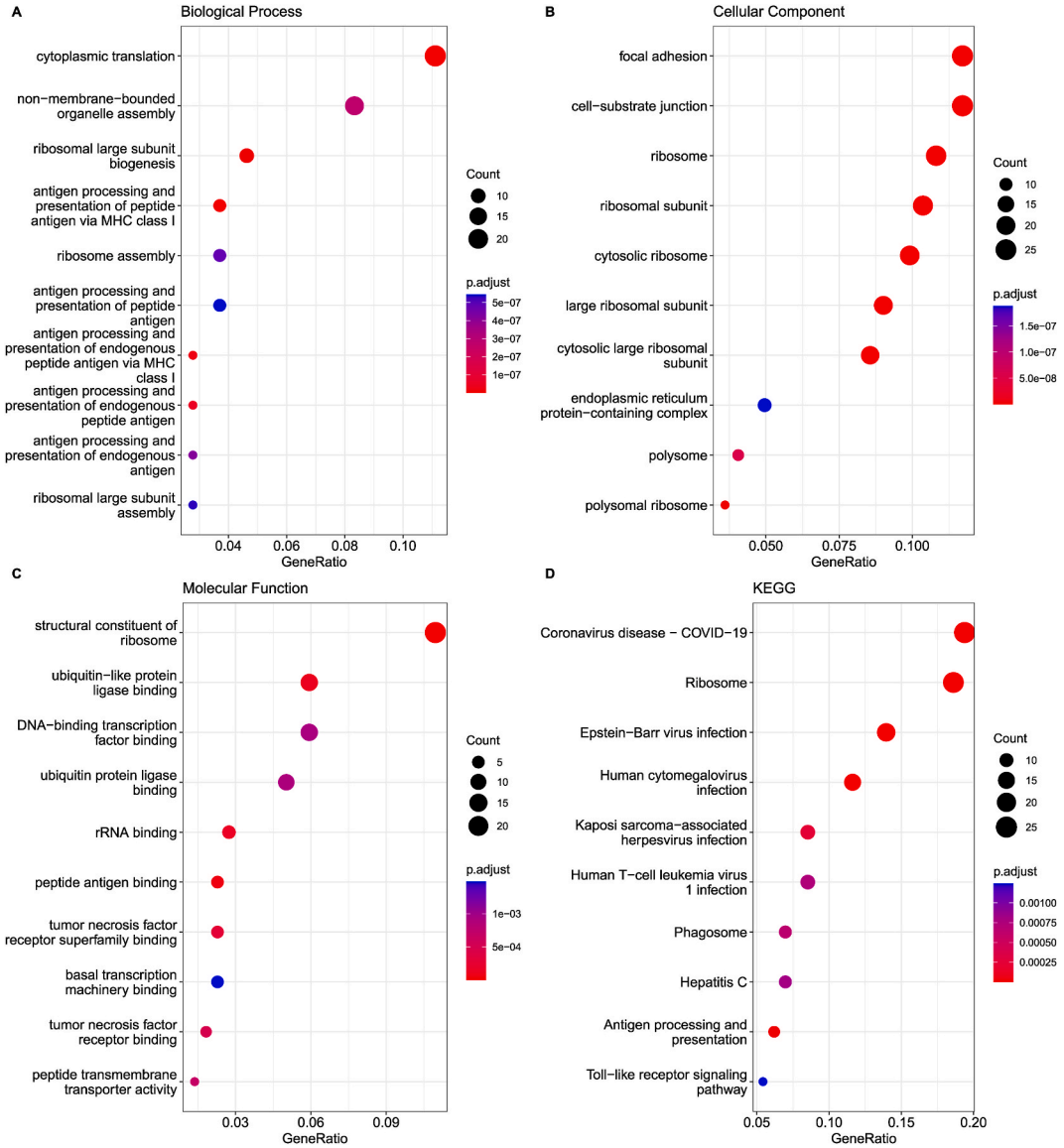

Fig. 2. Enrichment analyses of the differential GSTTKs.
A. Enrichment items of biological process category. B. Enrichment items of cellular component category. C. Enrichment items of molecular function category. D. Enrichment pathways of KEGG analysis.

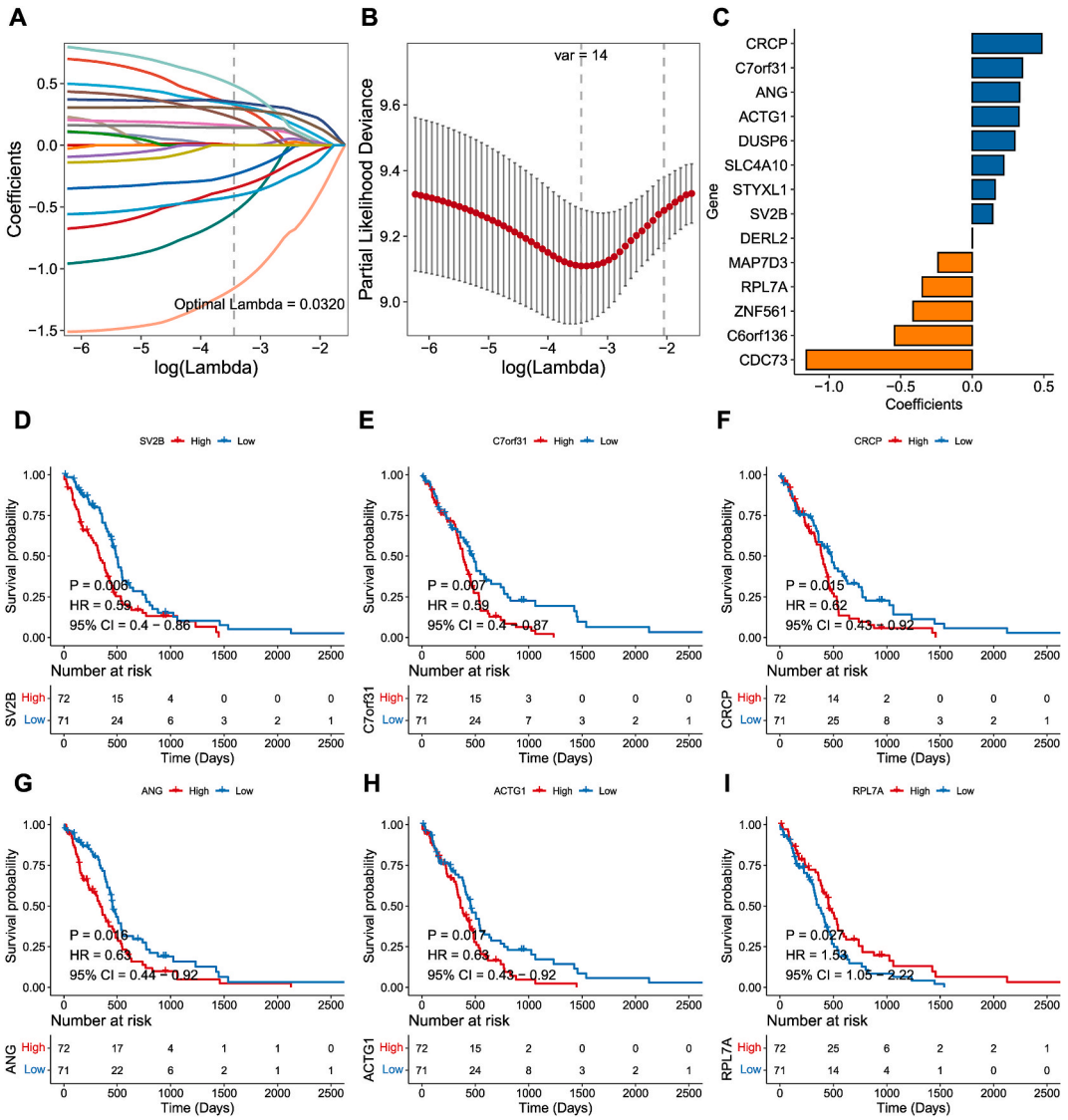

Fig. 3. LASSO Cox regression of prognosis-related GSTTKs and survival analysis.
A. LASSO coefficients of 20 prognosis-related GSTTKs. B. 95 % confidence interval of partial likelihood deviance though cross-validation. C. The coefficients of 14 optimal GSTTKs included into the TTK signature. D-I. Survival curves of the top six signature genes in TCGA-GBM samples.

Patients having a high-score exhibited a lower overall survival rate compared to those with low-scores (Fig. 4D). In the meantime, the AUC for the TTK signature in prediction of 1-, 3-, and 5-year survival was 0.776, 0.941, and 0.953, respectively (Fig. 4E). In order to assess the robustness of the TTK signature, the scores for every sample in the validation cohort were computed using the identical formula (Fig. 5A–C). In the GSE121720 cohort, patients with high scores exhibited a considerably more adverse prognosis compared to those with low scores (Fig. 5D). And the TTK signature had an accuracy of 0.612, 0.706, and 0.510 in predicting 1-, 3-, and 5-year survival, respectively (Fig. 5E).

3.3. Correlation between TTK signature and clinicopathological features

Afterwards, we examined the association between the TTK signature and the clinicopathological characteristics of GBM patients. No notable difference in the TTK scores was observed across subgroups based on age, gender, and original subtype (Fig. 6A, B, E). As expected, individuals with IDH-wildtype, and MGMT unmethylated exhibited higher scores in contrast to patients with IDH-mutant, and MGMT methylated, respectively (Fig. 6C and D). In the training cohort, we also analyzed the difference in progression-free interval and disease-specific survival between two groups. The Kaplan-Meier analysis revealed a significant correlation between high score and poorer PFI and DSS in patients with GBM (Supplementary Fig. S7).

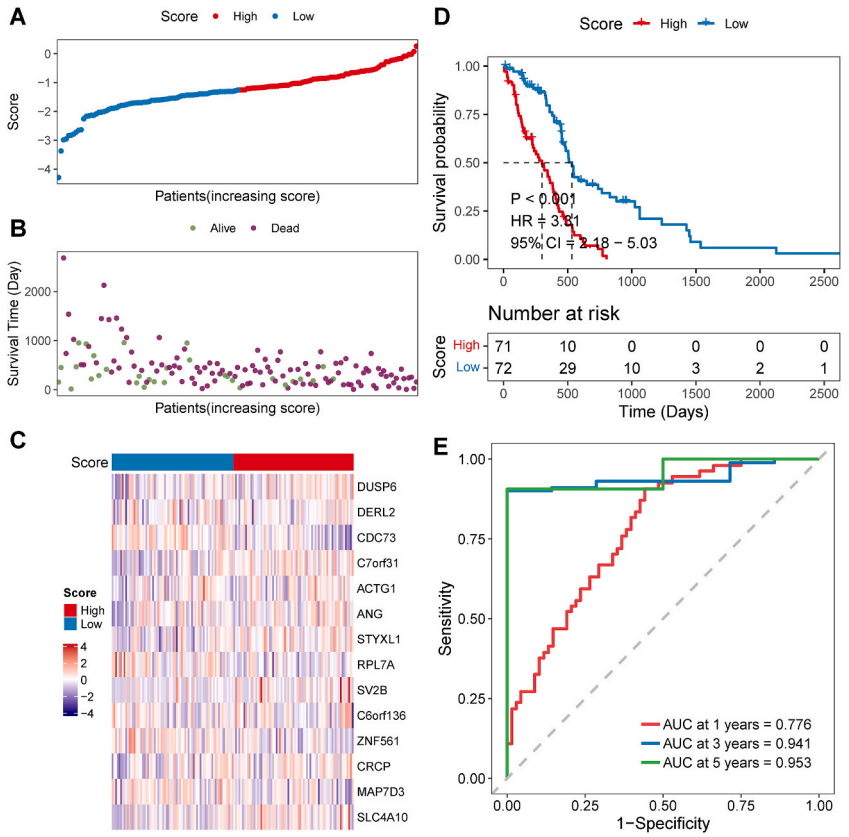

Fig. 4. Development of the TTK signature in GBM cohort from TCGA.
A. The distribution of TTK scores of every sample. B. The survival condition of each sample. C. The expression of 14 signature genes of every sample. D. Survival curve of OS for low-score and high-score groups divided by TTK signature. E. AUC of the TTK signature in predicting OS of GBM patients.

3.4. Establishment of the nomogram

In the TCGA-GBM cohort, the TTK signature, IDH status, and MGMT status were identified as prognostic factors with the univariate Cox analysis. Additionally, the multivariate Cox model provided further confirmation of the TTK signature's independent prognostic role (Fig. 7A). The TTK signature was identified as a robust prognostic indicator for GBM in the GSE121720 cohort, based on the findings from both univariate and multivariate models (Fig. 7B). Subsequently, we combined the TTK signature with age, gender, IDH status, and original subtype to create a comprehensive nomogram (Fig. 7C). The MGMT status was not integrated into the nomogram model since some data were not available. The nomogram predicted OS aligned with the actual OS, as demonstrated by the calibration curves (Fig. 7D). Additionally, the decision curve analysis suggested a significant potential for clinical practice of this nomogram (Fig. 7E).

3.5. TTK signature predicted the TME immune phenotypes

The initial step involved conducting ssGSEA analysis on the scores of immune cells. The results indicated a positive correlation between the TTK signature and the infiltration degree of immunocyte, such as central memory CD4 T cell, macrophage, monocyte, and natural killer cell (Fig. 8A). Next, we examined the relationship between the 14 signature genes and TTK score alongside 28 types of immunocyte. The findings demonstrated the MDSC, macrophage, central memory CD8 T cell, and natural killer T cell showed a significant positive correlation with ANG expression and TTK score, and significant negative correlation with C6orf136 expression (**Fig. 8B**). Moreover, a notable disparity was observed in the immune checkpoint expression levels between two groups, encompassing CD274 (PD-L1), CD226, CD40, LAIR1, and LGALS9 (Fig. 8C).

3.6. TTK signature predicted the immunotherapy response

The evaluation of the patients' reaction to ICIs treatment was conducted using the cohort associated with immunotherapy. In the beginning, the Kaplan-Meier analysis demonstrated a notable difference in the likelihood of survival between two groups (Fig. 9A). The TTK scores showed a notable disparity between patients who responded to immunotherapy and those who did not (Fig. 9B). The group

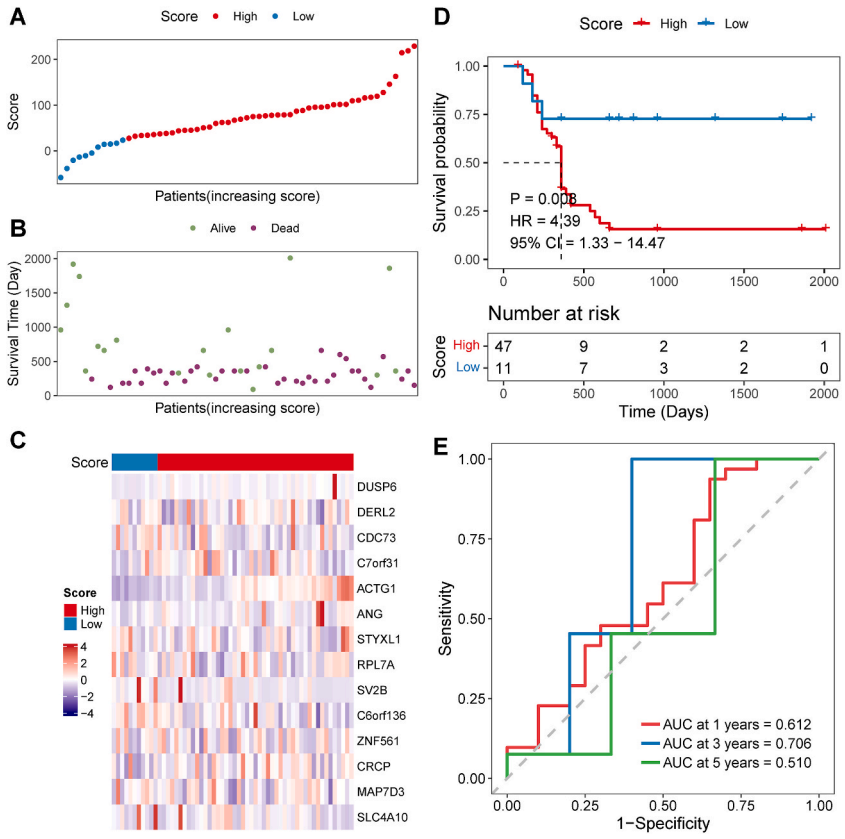

Fig. 5. Validation of the TTK signature in GBM cohort from GSE121720.
A. The distribution of TTK scores of every sample.B. The survival condition of each sample.C. The expression of 14 signature genes of every sample. D. Survival curve of OS for low-score and high-score groups classified by TTK signature.E. AUC of the TTK signature in predicting OS of GBM patients.

with lower scores had a greater percentage (91.67 %) of patients who could greatly benefit from immunotherapy compared to the group with higher scores (48.28 %) (Fig. 9C). The findings suggested that individuals with low scores exhibited higher rates of ICIs response and improved prognosis, despite the lack of statistical significance in TIDE score (Fig. 9D).

3.7. Molecular docking to screen candidate compounds

Data on the compounds' structure were obtained from the DrugBank database, resulting in a collection of 5462 small molecules that adhered to Lipinski's rules (with a hydrogen bond acceptor count of ten or less, hydrogen bond donor count of five or less, rotatable bond count of ten or less, logarithm of lipid water partition coefficient of five or less, molecular weight ranging from 180 to 480, and polar surface area of 140 or less). Out of the 14 signature genes, only ANG, CDC73, CRCP, DUSP6, and RPL7A possessed structural data in the PDB repository. Consequently, the corresponding PDB files 4AOH, 5YDE, 7AE1, 1 MKP, and 7F5S were acquired. Molecular docking calculations were performed with the AutoDock-Vina program and the interaction force were analyzed using Pymol and Ligplus. Table 1 and Fig. 10A–E displayed the top-performing small molecule compounds when combined with ANG, CDC73, CRCP, DUSP6, and RPL7A.

4. Discussion

The broad attention has been captured by the promising therapeutic benefits of ICIs for cancer treatment in recent years. Due to the "cold phenotype" of GBM and multiple therapy resistance, the clinical practice of ICIs in GBM patients remains challenging [12–14]. Hence, it is crucial to extensively investigate the distinctive immune condition of TME in GBM in order to expand the practical use of immunotherapy. The biomarkers with higher sensitivity for tracking the immune response could expedite the clinical advancement of efficient immunotherapy for patients with GBM [28–30].

Until now, there has been limited research on the impact of TTK associated signature to provide information for the prediction of GBM outcome. Our study identified the GSTTKs that were expressed differently between GBM samples and normal samples. Additionally, a TTK signature model, consisting of 14 optimal genes, was developed with LASSO algorithm. Based on the TTK signature

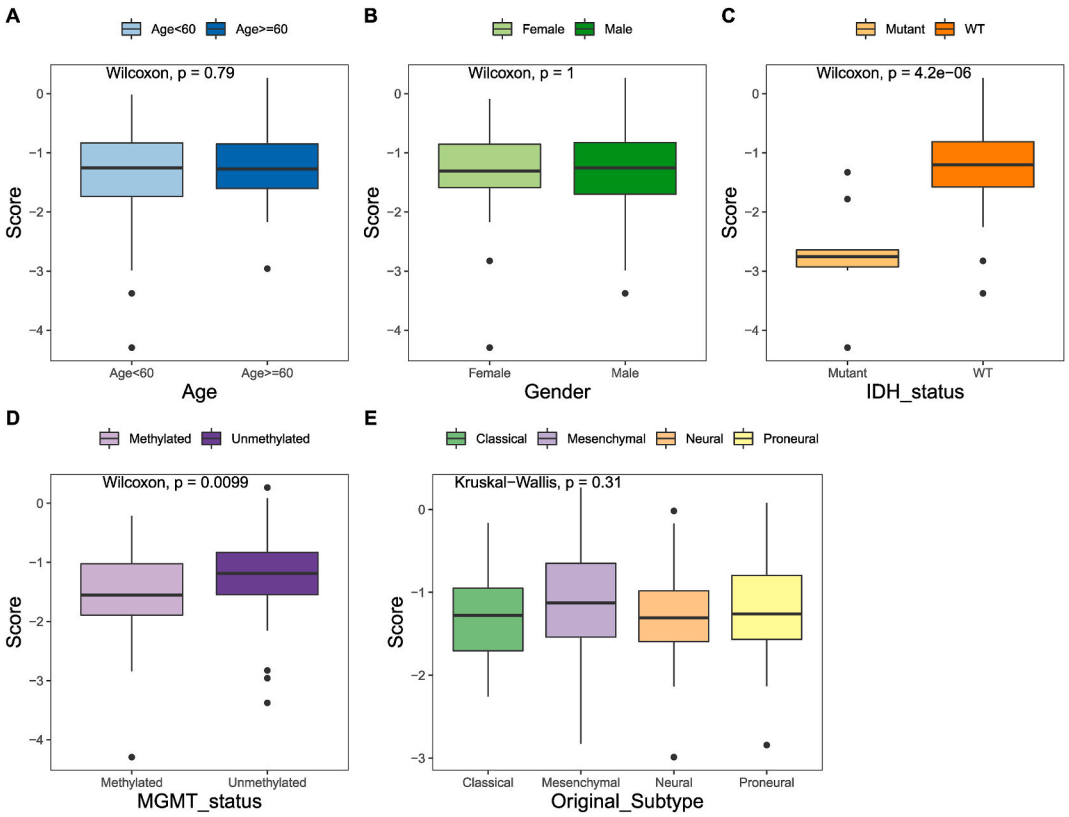

Fig. 6. TTK signature correlated the clinicopathological features of GBM.
A-E. Comparison of TTK scores difference between different GBM clinicopathological features, such as age, gender, IDH status, MGMT status, and original subtype.

model scores, the patients were categorized into groups with high or low scores. The GBM patients in the low-scoring group exhibited higher survival rates compared to those in the high-scoring group. The Cox regression analyses confirmed that the TTK signature we developed served as an independent prognostic indicator. These results was further strengthened by the independent validation cohort.

These signature genes included CRCP, C7orf31, ANG, ACTG1, DUSP6, SLC4A10, STYXL1, SV2B, DERL2, MAP7D3, RPL7A, ZNF561, C6orf136, and CDC73. Angiogenin (ANG) exerts potent stimulating effects on angiogenesis. The invasion, vascular connection, and proliferation of GBM cells were facilitated by ANG and its receptor plexin-B2 [31]. ANG upregulation was an unfavorable prognostic biomarker in the proneural subtype of GBM [32]. ANG, mainly expressed by tumor cells, was closely associated with the activity of antigen-presenting cells and macrophages in gliomas. In addition, higher ANG expression recruited mononuclear macrophage lineages and dendritic cells into the TME of glioma [33]. The localization of SV2B and other members of the SV2 protein family is in synaptic vesicles, and they may play a role in regulating vesicle trafficking, exocytosis, glucose transport, and energy metabolism. Additionally, the high expression of SV2B, providing nutrients to tumor cells and promoting tumor cell migration, has been correlated to poor survival in GBM [34]. ACTG1 functions as a vital part of the cytoskeleton and has a central role in maintaining cell survival. ACTG1 was overexpressed in GBM cells, and decreased ACTG1 inhibited proliferation and promoted apoptosis. COX10-AS1 acted as a sponge for miR-361–5p, leading to an increase in ACTG1 expression, which accelerating the development of cancer [35]. DUSP6 plays a vital role in controlling the ERK pathway and has been identified as a suppressor of tumor growth. Nevertheless, DUSP6 exhibited an unforeseen capacity to promote tumor growth in human GBM. This was achieved by contributing to the transition from epithelial to mesenchymal cells and the acquisition of an invasive phenotype [36]. GBM cells with high DUSP6 expression were resistant to cell death induced by cisplatin [37]. One study revealed that four genes, RPL7A, APOE, FN1, and GSTM2 significantly affected differentiation of GBM cells. Additionally, the survival analysis indicated that a decrease in RPL7A expression was linked to unfavorable OS among GBM patients [38]. C7orf31 was overexpressed in GBM, and was identified as a short-term survival-related gene [39]. STYXL1 was up-regulated in GBM and correlated to poor outcome. STYXL1 overexpression can promote glioma cell growth and migration [40]. CDC73 is a member of the cyclins family, which can prevent cell from growing and dividing too fast or out of control, and involves in tumorigenesis of GBM [41].

Afterwards, we analyzed the correlation between the TTK signature and clinicopathological features. Our findings indicated that patients with IDH-wildtype and MGMT unmethylation had a higher score than patients with IDH mutation and MGMT methylation. These results align with the adverse prognostic impact of the TTK model. Gliomas with mutated IDH and gliomas with wild IDH have

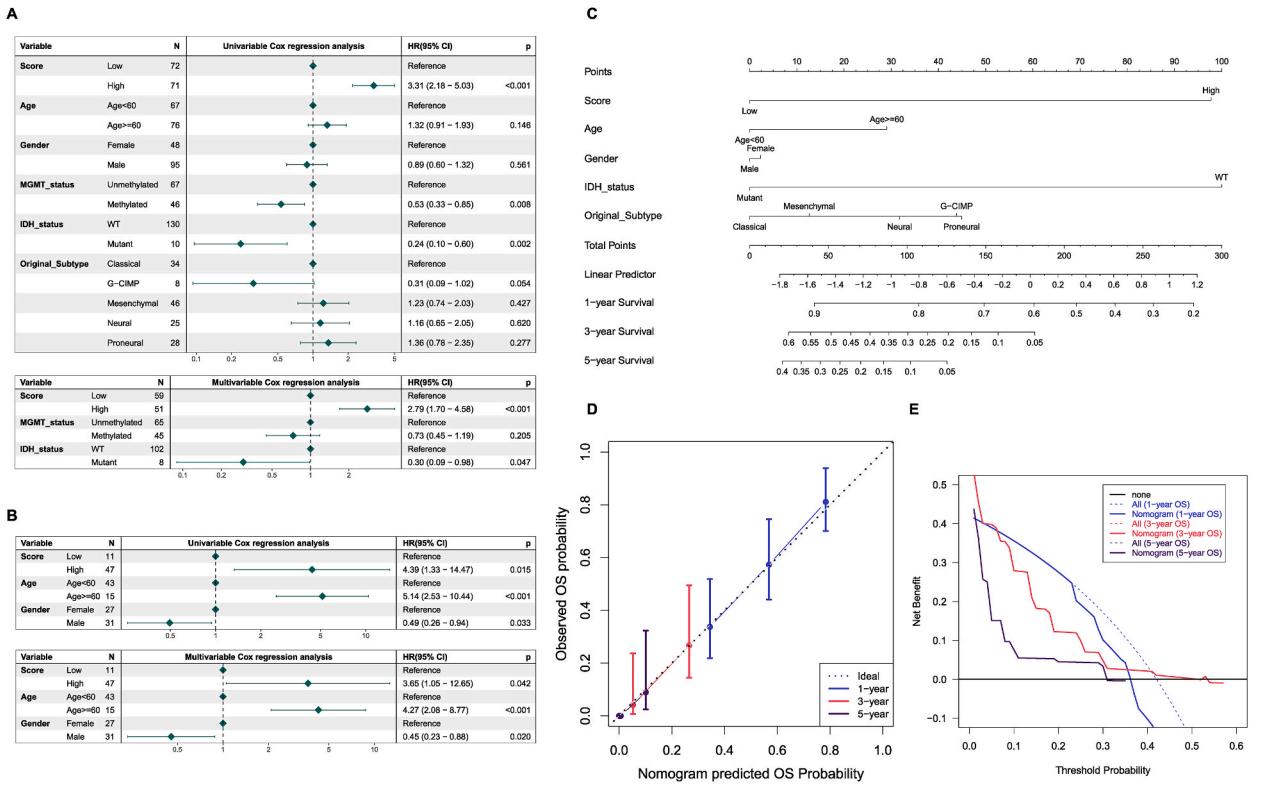

Fig. 7. Construction and evaluation of a comprehensive nomogram based on TTK signature.
A. Univariate and multivariate Cox models in TCGA-GBM cohort. B. Univariate and multivariate Cox models in GSE121720 cohort. C. Development of the nomogram containing TTK signature, gender, age, IDH status, and original subtype. D. The calibration plot of the constructed nomogram. E. The decision curve analysis of the constructed nomogram.

distinct tumor progression mechanisms, resulting in varied responses to treatments. Regardless of the grade or histology of glioma, patients with IDH-mutant gliomas exhibit a more favorable prognosis compared to those with IDH-wildtype [42]. Several clinical trials have indicated that the methylation of MGMT promoter is a reliable predictor of improved outcome in GBM [43]. The potential mechanism that leads to longer OS could be the reduced DNA repair caused by promoter methylation-induced silencing of the MGMT gene [44]. In the present investigation, the Kaplan-Meier analysis also demonstrated a correlation between a higher score and poorer PFI and DSS in patients with GBM.

Additionally, we also attempted to explore the relationship between TTK model and immune phenotypes in the TME. Initially, the TTK signature exhibited a strong association with the infiltration degree of immunocyte, such as central memory CD4 T cells, macrophages, monocytes, and natural killer cells. Nevertheless, the findings also indicated a positive association between the TTK score and Tregs and myeloid-derived suppressor cells, which were deemed as inhibitors of anticancer immunity [45]. Therefore, the existing anticancer effects of individuals with high-score might be limited due to the increased presence of Tregs and myeloid-derived suppressor cells. Furthermore, the TTK signature exhibited a strong positive correlation with the immune checkpoint expression levels, encompassing PD-L1, CD226, CD40, LAIR1, and LGALS9. Moreover, macrophage, MDSC, the central memory CD4 T cell, and natural killer T cell exhibited a notable positive connection with ANG expression and TTK score, while displaying a significant negative relationship with C6orf136 expression. These findings indicate that ANG was a risk gene and C6orf136 was a protective gene in GBM.

Furthermore, the survival analysis in the immunotherapy cohort found that patients in the high-scoring group exhibited lower survival rates, aligning with the findings from our TTK signature model. Patients with a low score exhibited higher response rates to ICIs and a more favorable prognosis, indicating that the TTK model may potentially act as a tool for tailoring immunotherapy to individualize treatment for GBM in the future. The process of molecular docking was conducted to choose small molecule compounds that target proteins encoded by signature genes. Specifically, DB15345, DB07507, DB06985, DB12821, and DB08049 were the selected compounds. These small molecules would be good candidates to be developed as drugs against GBM.

Several prognostic and personalized treatment prediction models for GBM have been developed, focusing on ferroptosis, pyroptosis, autophagy, and glucose metabolism [46–48]. A published study has examined the prediction of TTK signature in liver cancer [49]. This study initially screened the best candidate genes from a large number of GSTTKs using various algorithms. Furthermore, we created a 14-gene signature and examined its association with clinicopathological characteristics, immune phenotypes, and treatment effectiveness. Next, we verified our TTK model in an external group. There were, however, some limitations to our study. First, all of our findings were relying on information sourced from the public database. Additional biological experiments will be required to

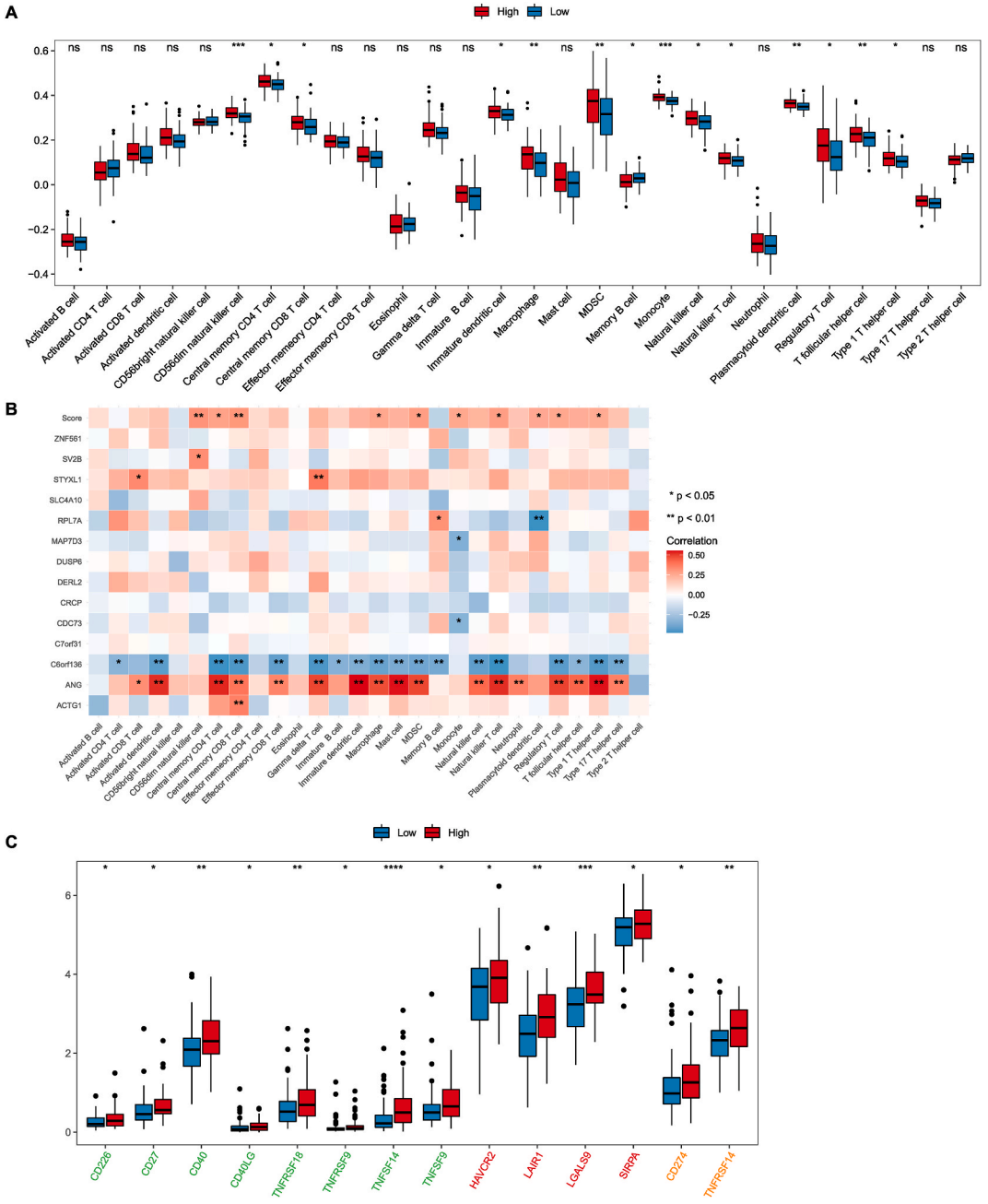

Fig. 8. Relationships between the TTK signature and immune states.
A. Relationships between the TTK signature and the infiltration scores of 28 types of immune cells. B. The correlation between the 14 signature genes and TTK score and different immune cells. C. The significant difference in expression of immune checkpoint. Active genes were shown in green, inhibit genes were shown in red, and two side genes were shown in orange. (For interpretation of the references to colour in this figure legend, the reader is referred to the Web version of this article.)

elucidate the mechanisms involved, even though we also verified these findings in the GEO cohort. Furthermore, we only utilized a single external cohort to verify the accuracy of our findings. Additional data with a substantial sample size are necessary to further validate the TTK signature. Third, further investigation is required to explore the potential use of the TTK signature in clinical settings. In addition, the efficacy of small molecule compounds screened by molecular docking should also be verified by biomedical experiments in the future.

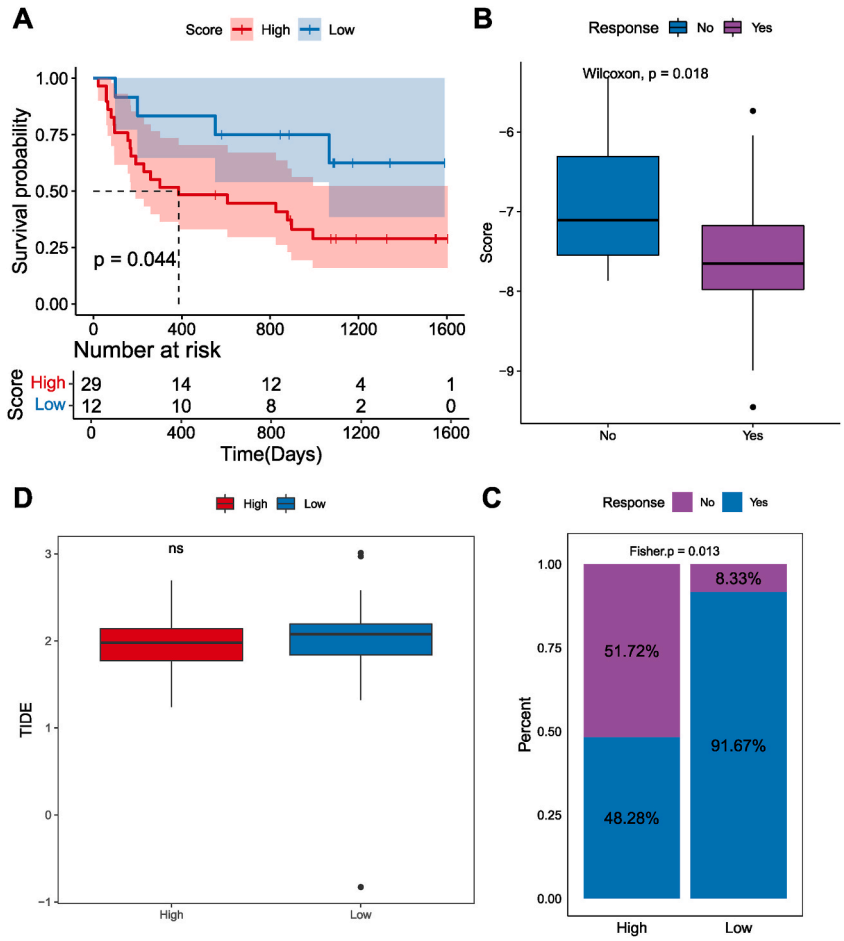

Fig. 9. TTK signature correlated the response to immunotherapy.
A. Kaplan-Meier survival difference between two score groups. B. Comparison of TTK scores in patients with and without response to immunotherapy. C. Proportion of patients with and without response to immunotherapy. D. Comparison of TIDE score among the two score groups.

Table 1
The compounds with the best docking scores against each target protein.

Protein	DrugBank_ID	Hydrogen Acceptors	Hydrogen Donors	Rotatable Bonds	LogP	Molecular Weight	TPSA	Affinity (kcal/mol)
ANG	DB15345	8	1	5	1.1	451.5	79.8	−8.5
CDC73	DB07507	3	1	2	4.1	329.3	57.6	−8.4
CRCP	DB06985	6	2	3	4.3	392.4	69.6	−8.6
DUSP6	DB12821	10	0	1	3.8	238.03	0	−6.1
RPL7A	DB08049	4	2	1	2.4	254.24	66.8	−7.4

TPSA, topology polar surface area.

5. Conclusion

In summary, we built a TTK signature that has an independent predictive value for GBM prognosis. Patients who had a high score experienced a more unfavorable prognosis. The close relationship between the TTK signature and clinicopathological features, as well as the immune phenotypes of TME, was observed. Additionally, it predicted the therapeutic efficacy of immunotherapy for GBM.

Data availability statement

The datasets used in this study are available in TCGA or GEO database under accession number GSE121720.

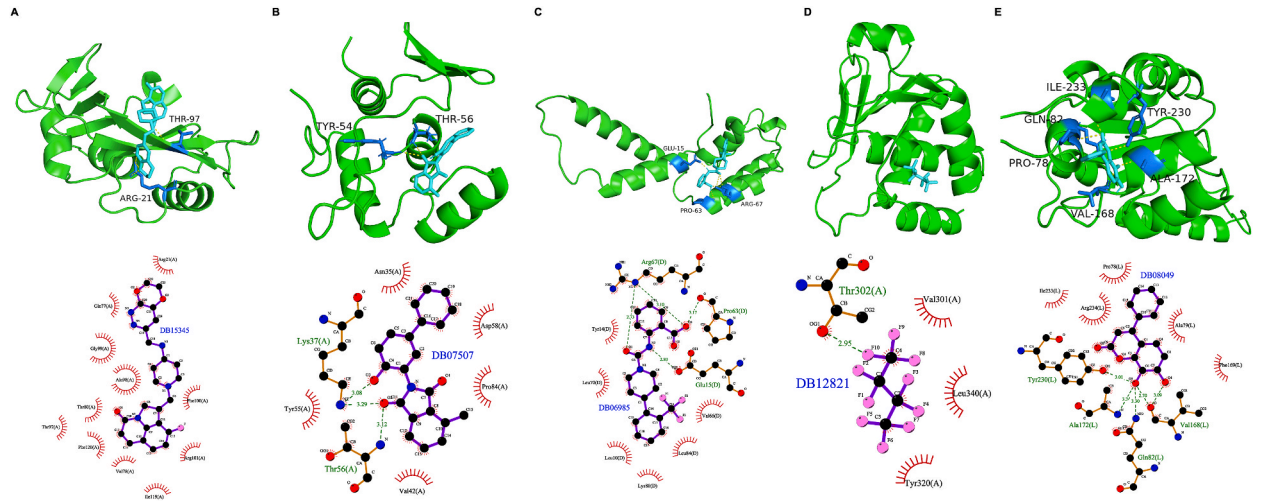

Fig. 10. Molecular docking of compounds against target proteins.
A-E. The docking conformation and interaction force between DB15345 and ANG protein, DB07507 and CDC73 protein, DB06985 and CRCP protein, DB12821 and DUSP6 protein, DB08049 and RPL7A protein. The upper part: Pymol displayed the docking conformation and hydrogen bond. The cyan represented small molecule, the yellow dotted line represented hydrogen bond, and the blue represented amino acid residue forming hydrogen bond with small molecule. The lower part: Ligplus force analysis. Small molecules located in the center, surrounded by amino acid residues. The green dotted line represented hydrogen bond, green amino acid name represented amino acid residue forming hydrogen bond with small molecule. (For interpretation of the references to colour in this figure legend, the reader is referred to the Web version of this article.)

Funding

This research was funded by the Medical Key Cultivation Discipline Program of Luoyang (No. STE-2022-5).

CRediT authorship contribution statement

Hongchao Liu: Writing – review & editing, Writing – original draft, Visualization, Validation, Project administration, Investigation, Formal analysis, Conceptualization. **Kangke Shi:** Validation, Software, Methodology, Formal analysis. **Zhihao Wei:** Visualization, Validation, Software, Project administration, Methodology, Funding acquisition, Conceptualization. **Yu Zhang:** Writing – review & editing, Visualization, Validation, Software, Resources, Data curation. **Jiaqiong Li:** Software, Resources, Methodology, Investigation, Formal analysis, Data curation, Conceptualization.

Declaration of competing interest

The authors declare that they have no known competing financial interests or personal relationships that could have appeared to influence the work reported in this paper.

Appendix A. Supplementary data

Supplementary data to this article can be found online at https://doi.org/10.1016/j.heliyon.2024.e31207.

References

[1] A. Urbaniak, M.R. Reed, B. Heflin, J. Gaydos, S. Piña-Oviedo, M. Jędrzejczyk, G. Klejborowska, N. Stępczyńska, T.C. Chambers, A.J. Tackett, A. Rodriguez, A. Huczyński, R.L. Eoff, et al., Anti-glioblastoma activity of monensin and its analogs in an organoid model of cancer, Biomed. Pharmacother. 153 (2022) 113440.
[2] T.I. Janjua, P. Rewatkar, A. Ahmed-Cox, I. Saeed, F.M. Mansfeld, R. Kulshreshtha, T. Kumeria, D.S. Ziegler, M. Kavallaris, R. Mazzieri, A. Popat, Frontiers in the treatment of glioblastoma: past, present and emerging, Adv. Drug Deliv. Rev. 171 (2021) 108–138.
[3] E. Le Rhun, M. Preusser, P. Roth, D.A. Reardon, M. van den Bent, P. Wen, G. Reifenberger, M. Weller, Molecular targeted therapy of glioblastoma, Cancer Treat Rev. 80 (2019) 101896.
[4] E. Tirrò, M. Massimino, C. Romano, F. Martorana, M.S. Pennisi, S. Stella, G. Pavone, S. Di Gregorio, A. Puma, C. Tomarchio, S.R. Vitale, L. Manzella, P. Vigneri, Prognostic and therapeutic roles of the insulin growth factor system in glioblastoma, Front. Oncol. 10 (2020) 612385.
[5] R. Liu, X.-P. Qin, Y. Zhuang, Y. Zhang, H.-B. Liao, J.-C. Tang, M.-X. Pan, F.-F. Zeng, Y. Lei, R.-X. Lei, S. Wang, A.-C. Liu, J. Chen, et al., Glioblastoma recurrence correlates with NLGN3 levels, Cancer Med. 7 (2018) 2848–2859.
[6] F. Zhou, M. Qiao, C. Zhou, The cutting-edge progress of immune-checkpoint blockade in lung cancer, Cell. Mol. Immunol. 18 (2021) 279–293.

[7] F. Sabbatino, L. Liguori, S. Pepe, S. Ferrone, Immune checkpoint inhibitors for the treatment of melanoma, Expet Opin. Biol. Ther. 22 (2022) 563–576.
[8] B. Huang, X. Li, Y. Li, J. Zhang, Z. Zong, H. Zhang, Current immunotherapies for glioblastoma multiforme, Front. Immunol. 11 (2020) 603911.
[9] M.S. Carlino, J. Larkin, G.V. Long, Immune checkpoint inhibitors in melanoma, Lancet. 398 (2021) 1002–1014.
[10] F. Petitprez, M. Meylan, A. de Reyniès, C. Sautès-Fridman, W.H. Fridman, The tumor microenvironment in the response to immune checkpoint blockade therapies, Front. Immunol. 11 (2020) 784.
[11] B. Farhood, M. Najafi, K. Mortezaee, CD8+ cytotoxic T lymphocytes in cancer immunotherapy: a review, J. Cell. Physiol. 234 (2019) 8509–8521.
[12] S. DeCordova, A. Shastri, A.G. Tsolaki, H. Yasmin, L. Klein, S.K. Singh, U. Kishore, Molecular heterogeneity and immunosuppressive microenvironment in glioblastoma, Front. Immunol. 11 (2020) 1402.
[13] L. Gong, L. Ji, D. Xu, J. Wang, J. Zou, TGF-β links glycolysis and immunosuppression in glioblastoma, Histol. Histopathol. 36 (2021) 1111–1124.
[14] R. Medikonda, G. Dunn, M. Rahman, P. Fecci, M. Lim, A review of glioblastoma immunotherapy, J. Neuro Oncol. 151 (2021) 41–53.
[15] A. Colaprico, T.C. Silva, C. Olsen, L. Garofano, C. Cava, D. Garolini, T.S. Sabedot, T.M. Malta, S.M. Pagnotta, I. Castiglioni, M. Ceccarelli, G. Bontempi, H. Noushmehr, TCGAbiolinks: an R/Bioconductor package for integrative analysis of TCGA data, Nucleic Acids Res. 44 (2016) e71.
[16] Y. Wu, M. Fletcher, Z. Gu, Q. Wang, B. Costa, A. Bertoni, K.-H. Man, M. Schlotter, J. Felsberg, J. Mangei, M. Barbus, A.-C. Gaupel, W. Wang, et al., Glioblastoma epigenome profiling identifies SOX10 as a master regulator of molecular tumour subtype, Nat. Commun. 11 (2020) 6434.
[17] B. Ru, C.N. Wong, Y. Tong, J.Y. Zhong, S.S.W. Zhong, W.C. Wu, K.C. Chu, C.Y. Wong, C.Y. Lau, I. Chen, N.W. Chan, J. Zhang, TISIDB: an integrated repository portal for tumor-immune system interactions, Bioinformatics 35 (2019) 4200–4202.
[18] M.E. Ritchie, B. Phipson, D. Wu, Y. Hu, C.W. Law, W. Shi, G.K. Smyth, Limma powers differential expression analyses for RNA-sequencing and microarray studies, Nucleic Acids Res. 43 (2015) e47.
[19] T. Wu, E. Hu, S. Xu, M. Chen, P. Guo, Z. Dai, T. Feng, L. Zhou, W. Tang, L. Zhan, X. Fu, S. Liu, X. Bo, et al., clusterProfiler 4.0: a universal enrichment tool for interpreting omics data, Innovation 2 (2021) 100141.
[20] D. Szklarczyk, A.L. Gable, K.C. Nastou, D. Lyon, R. Kirsch, S. Pyysalo, N.T. Doncheva, M. Legeay, T. Fang, P. Bork, L.J. Jensen, C. von Mering, The STRING database in 2021: customizable protein-protein networks, and functional characterization of user-uploaded gene/measurement sets, Nucleic Acids Res. 49 (2021) D605–D612.
[21] M. Zhang, K. Zhu, H. Pu, Z. Wang, H. Zhao, J. Zhang, Y. Wang, An immune-related signature predicts survival in patients with lung adenocarcinoma, Front. Oncol. 9 (2019) 1314.
[22] L. Liang, J. Yu, J. Li, N. Li, J. Liu, L. Xiu, J. Zeng, T. Wang, L. Wu, Integration of scRNA-seq and bulk RNA-seq to analyse the heterogeneity of ovarian cancer immune cells and establish a molecular risk model, Front. Oncol. 11 (2021) 711020.
[23] P. Charoentong, F. Finotello, M. Angelova, C. Mayer, M. Efremova, D. Rieder, H. Hackl, Z. Trajanoski, Pan-cancer immunogenomic analyses reveal genotype-immunophenotype relationships and predictors of response to checkpoint blockade, Cell Rep. 18 (2017) 248–262.
[24] T.N. Gide, C. Quek, A.M. Menzies, A.T. Tasker, P. Shang, J. Holst, J. Madore, S.Y. Lim, R. Velickovic, M. Wongchenko, Y. Yan, S. Lo, M.S. Carlino, et al., Distinct immune cell populations define response to anti-PD-1 monotherapy and anti-PD-1/anti-CTLA-4 combined therapy, Cancer Cell 35 (2019) 238–255.e6.
[25] P. Jiang, S. Gu, D. Pan, J. Fu, A. Sahu, X. Hu, Z. Li, N. Traugh, X. Bu, B. Li, J. Liu, G.J. Freeman, M.A. Brown, et al., Signatures of T cell dysfunction and exclusion predict cancer immunotherapy response, Nat Med 24 (2018) 1550–1558.
[26] J. Liu, F. Zhang, J. Zhong, Z. Zheng, Signature and molecular mechanism of mitochondrial energy metabolism pathway-related genes in lung adenocarcinoma, Dis. Markers 2022 (2022) 3201600.
[27] D. Seeliger, B.L. de Groot, Ligand docking and binding site analysis with PyMOL and Autodock/Vina, J. Comput. Aided Mol. Des. 24 (2010) 417–422.
[28] A. Ghouzlani, S. Kandoussi, M. Tall, K.P. Reddy, S. Rafii, A. Badou, Immune checkpoint inhibitors in human glioma microenvironment, Front. Immunol. 12 (2021) 679425.
[29] J.P. Lynes, A.K. Nwankwo, H.P. Sur, V.E. Sanchez, K.A. Sarpong, O.I. Ariyo, G.A. Dominah, E.K. Nduom, Biomarkers for immunotherapy for treatment of glioblastoma, J Immunother Cancer 8 (2020) e000348.
[30] J. Zhao, A.X. Chen, R.D. Gartrell, A.M. Silverman, L. Aparicio, T. Chu, D. Bordbar, D. Shan, J. Samanamud, A. Mahajan, I. Filip, R. Orenbuch, M. Goetz, et al., Immune and genomic correlates of response to anti-PD-1 immunotherapy in glioblastoma, Nat Med 25 (2019) 462–469.
[31] H. Yang, L. Yuan, S. Ibaragi, S. Li, R. Shapiro, N. Vanli, K.A. Goncalves, W. Yu, H. Kishikawa, Y. Jiang, A.J. Hu, D. Jay, B. Cochran, et al., Angiogenin and plexin-B2 axis promotes glioblastoma progression by enhancing invasion, vascular association, proliferation and survival, Br. J. Cancer 127 (2022) 422–435.
[32] J.-L. Hu, W.-J. Luo, H. Wang, Angiogenin upregulation independently predicts unfavorable overall survival in proneural subtype of glioblastoma, Technol. Cancer Res. Treat. 18 (2019) 1533033819846636.
[33] J. Wang, J.-A. Shan, F. Shi, Q. Zheng, Molecular and clinical characterization of ANG expression in gliomas and its association with tumor-related immune response, Front. Med. 10 (2023) 1044402.
[34] Y. Zhang, X. Yang, X.-L. Zhu, J.-Q. Hao, H. Bai, Y.-C. Xiao, Z.-Z. Wang, C.-Y. Hao, H.-B. Duan, Bioinformatics analysis of potential core genes for glioblastoma, Biosci. Rep. 40 (2020) BSR20201625.
[35] C. Zhou, X. Jiang, A. Liang, R. Zhu, Y. Yang, L. Zhong, D. Wan, COX10-AS1 facilitates cell proliferation and inhibits cell apoptosis in glioblastoma cells at post-transcription level, Neurochem. Res. 45 (2020) 2196–2203.
[36] C. Zuchegna, E. Di Zazzo, B. Moncharmont, S. Messina, Dual-specificity phosphatase (DUSP6) in human glioblastoma: epithelial-to-mesenchymal transition (EMT) involvement, BMC Res. Notes 13 (2020) 374.
[37] S. Messina, L. Frati, C. Leonetti, C. Zuchegna, E. Di Zazzo, A. Calogero, A. Porcellini, Dual-specificity phosphatase DUSP6 has tumor-promoting properties in human glioblastomas, Oncogene 30 (2011) 3813–3820.
[38] Z. Wang, X. Guo, L. Gao, Y. Wang, W. Ma, B. Xing, Glioblastoma cell differentiation trajectory predicts the immunotherapy response and overall survival of patients, Aging (Albany NY) 12 (2020) 18297–18321.
[39] S. Liu, Y. Xu, S. Zhang, LINGO1, C7orf31 and VEGFA are prognostic genes of primary glioblastoma: analysis of gene expression microarray, Neoplasma 65 (2018) 532–541.
[40] V.S. Tomar, T.K. Baral, K. Nagavelu, K. Somasundaram, Serine/threonine/tyrosine-interacting-like protein 1 (STYXL1), a pseudo phosphatase, promotes oncogenesis in glioma, Biochem. Biophys. Res. Commun. 515 (2019) 241–247.
[41] M. Zhang, Z. Zhou, Z. Liu, F. Liu, C. Zhao, Exploring the potential biomarkers for prognosis of glioblastoma via weighted gene co-expression network analysis, PeerJ 10 (2022) e12768.
[42] K. Aldape, G. Zadeh, S. Mansouri, G. Reifenberger, A. von Deimling, Glioblastoma: pathology, molecular mechanisms and markers, Acta Neuropathol. 129 (2015) 829–848.
[43] M.M. Binabaj, A. Bahrami, S. ShahidSales, M. Joodi, M. Joudi Mashhad, S.M. Hassanian, K. Anvari, A. Avan, The prognostic value of MGMT promoter methylation in glioblastoma: a meta-analysis of clinical trials, J. Cell. Physiol. 233 (2018) 378–386.
[44] L. Morandi, E. Franceschi, D. de Biase, G. Marucci, A. Tosoni, M. Ermani, A. Pession, G. Tallini, A. Brandes, Promoter methylation analysis of O6-methylguanine-DNA methyltransferase in glioblastoma: detection by locked nucleic acid based quantitative PCR using an imprinted gene (SNURF) as a reference, BMC Cancer 10 (2010) 48.
[45] E.D. Kramer, S.I. Abrams, Granulocytic myeloid-derived suppressor cells as negative regulators of anticancer immunity, Front. Immunol. 11 (2020) 1963.
[46] X. Zhu, Y. Zhou, Y. Ou, Z. Cheng, D. Han, Z. Chu, S. Pan, Characterization of ferroptosis signature to evaluate the predict prognosis and immunotherapy in glioblastoma, Aging (Albany NY) 13 (2021) 17655–17672.

[47] J. Lin, X. Lai, X. Liu, H. Yan, C. Wu, Pyroptosis in glioblastoma: a crucial regulator of the tumour immune microenvironment and a predictor of prognosis, J. Cell Mol. Med. 26 (2022) 1579–1593.
[48] C. Zhang, M. Wang, F. Ji, Y. Peng, B. Wang, J. Zhao, J. Wu, H. Zhao, A novel glucose metabolism-related gene signature for overall survival prediction in patients with glioblastoma, BioMed Res. Int. 2021 (2021) 8872977.
[49] W.-F. Hong, M.-Y. Liu, L. Liang, Y. Zhang, Z.-J. Li, K. Han, S.-S. Du, Y.-J. Chen, L.-H. Ma, Molecular characteristics of T cell-mediated tumor killing in hepatocellular carcinoma, Front. Immunol. 13 (2022) 868480.